Optimised periodic and hyperchaotic modes of a triple pendulum

André E Botha[1] and Guoyuan Qi[2]

[1]Department of Physics, University of South Africa, P.O. Box 392, Pretoria 0003, South Africa
[2]F'SATI and Department of Electrical Engineering, Tshwane University of Technology,
 Private Bag X680, Pretoria 0001, South Africa

E-mail: `bothaae@unisa.ac.za, qig@tut.ac.za`

Abstract. Analytical equations of motion, in the form $\dot{\mathbf{x}} = f(\mathbf{x}, t)$, were derived for a damped harmonically driven triple plane pendulum. This form of the equations displayed the nature of the non-linear coupling and provided a basis for physical interpretation. It also facilitated the derivation of the Jacobian matrix in analytical form, an essential result for the accurate numerical computation of Lyapunov exponents. Sets of optimised initial conditions and parameters were derived by applying Nelder-Mead simplex optimisation to the calculated Lyapunov exponents. As an example of the method, it was used to calculate the initial conditions for a periodic mode of the un-damped pendulum. It was also used to demonstrate that the maximum Lyapunov exponent of the pendulum could be made to vary from zero, for a periodic mode, to above ten, for a hyperchaotic mode. Numerical simulations were coded in Python and used to visualise the results.

1. Introduction

Pendulums of varying complexity, ranging from the textbook example of a simple pendulum to much more complicated coupled systems, play an important role in mechanics, mainly because they illustrate interesting nonlinear dynamical effects in ways that often can be analysed mathematically. Although it is not well known, chaotic dynamics can even be observed in a simple pendulum, when it is externally excited [1].

Recently there have been a number of experimental and theoretical investigations aimed at understanding the stability of human gait (manner of stepping) through the use of inverted pendulum models [2, 3]. A number of experimental investigations of either simple or coupled electro-mechanically driven pendulums have also been undertaken, with the view of developing more precise conditions for the onset of chaos in these systems [4, 5]. On the technological front, a triple pendulum suspension system has been used to seismically isolate optical components on the GEO 600 interferometric gravitational wave detector [6]. This invention has allowed the detector to achieve a seismic noise sensitivity level which is well below the level from thermal noise.

Coupled pendulums with obstacles have been used to model real mechanical systems that exhibit nonlinear phenomena such as resonances, jumps between different system states, various continuous and discontinuous bifurcations, symmetry breaking and crisis bifurcations, pools of attractions, oscillatory-rotational attractors, etc. In reference [7], for example, it is shown that a triple pendulum model can provide insight into the real, highly-complicated dynamics of a

piston connecting-rod crankshaft system. In view of the limited space available for the present article, it is not possible to provide a complete review of related work. A more comprehensive review may be found in reference [8].

Although the triple pendulum has been the subject of an ongoing investigation by Awrejcewicz *et al.* [1, 8, 9] and Kudra [10], the chaotic and hyperchaotic regimes of the pendulum have yet to be fully explored. In previous work, such as [9], the highest two positive Lyapunov exponents were reported to be 0.06 and 0.01 (see table 2 of reference [9]). Since the chaos-hyperchaos transition is defined by when the second Lyapunov exponent becomes positive, Awrejcewicz *et al.* [9] correctly classify the attractor as hyperchaotic; however, it the present work it will be shown that in fact much higher values for the maximum Lyapunov exponent (above ten) are possible through optimisation.

This paper is organised as follows. In section 2, the equations for a triple pendulum are derived in a form that is well suited for the analysis of chaotic dynamics and for the use of optimisation. In section 3, details of the computational implementation of the optimisation calculation and visualisation are presented. Preliminary results for optimised periodic and hyperchaotic modes of the pendulum are presented in section 4. In the concluding section 5, it is noted that optimisation may provide a useful way of controlling the degree of chaos in non-linear dynamical systems. The method developed here for the pendulum could thus find applications in other non-linear systems ranging from biophysics to information technology.

2. Theory and analysis of the governing equations

Figure 1 shows a visualisation of the triple plane pendulum. It was generated from a screen-shot of a three-dimensional animation of the pendulum, created by using the *Visual* module in the *Python* programming language [11]. The pendulum consists of a series of absolutely rigid bars which form the three links of the pendulum (shown in red, green and blue). Additional point-like masses are attached to the bottom of each link (shown in yellow).
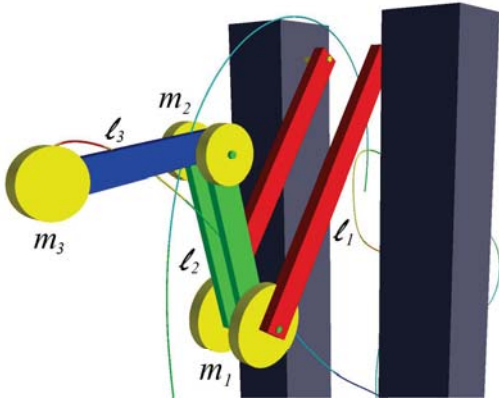
Figure 1. Visualisation of the triple plane pendulum. The pendulum is made of absolutely rigid bars (two of length ℓ_1, two of length ℓ_2 and one of length ℓ_3) to which cylindrical point-like masses are attached (two of mass $\frac{m_1}{2}$, two of mass $\frac{m_2}{2}$ and one of mass m_3). The pendulum is assumed to be under the influence of gravity and in vacuum. The three pivot points may exert viscous damping, with coefficients c_1, c_2 and c_3. Also shown in the figure is the trajectory followed by the centre of m_3.

The governing equations for the triple plane pendulum have been derived in reference [9]. They have the following matrix form:

$$\mathbf{M}(\boldsymbol{\psi})\ddot{\boldsymbol{\psi}} + \mathbf{B}(\boldsymbol{\psi})\dot{\boldsymbol{\psi}}^2 + \mathbf{C}\dot{\boldsymbol{\psi}} + \mathbf{D}(\boldsymbol{\psi}) = \mathbf{F}(t) \tag{1}$$

Equation (1) is written in the notation of reference [9], in which the angles between the vertical and each link of the pendulum are denoted by ψ_i $(i = 1, 2, 3)$, with $\boldsymbol{\psi} = (\psi_1, \psi_2, \psi_3)^{\mathrm{T}}$.

Instead of retaining the form of equation (1), a computer algebra system, *Maple 11*, was used to invert the matrix $\mathbf{M}$ in order to solve for $\ddot{\boldsymbol{\psi}}$. By then making the substitutions $x_1 = \psi_1$, $x_2 = \psi_2$, $x_3 = \psi_3$, $x_4 = \dot{\psi}_1$, $x_5 = \dot{\psi}_2$, and $x_6 = \dot{\psi}_3$, the equivalent first order system:

$$\dot{\mathbf{x}} = f(\mathbf{x}, t) \tag{2}$$

was obtained. Equations (2) are given explicitly in in Appendix A. Having analytical expressions for the governing equations in the form of (2) presents two important advantages.

Firstly, it can provide insight into the unusual nature of the non-linear coupling in this system. If one performs a power series expansion of the factor $1/D$ on right hand side of equations (A.4) to (A.6), one sees that the masses are coupled by terms involving products of sine and cosine functions (which are bounded by ± 1) with either constants or terms linear or quadratic in x_4 to x_6. Since x_4 to x_6 represent the angular speeds of the pendulum links, the increase in non-linear coupling is fundamentally limited by the total amount of mechanical energy stored in the pendulum. For a fixed amount of energy; however, the maximal coupling will be determined by the values of the physical parameters m_i and ℓ_i. In particular, one notices that all the coupling terms are inversely proportional to one of the three lengths, so that the coupling can be increased indefinitely by reducing one of the lengths. This is not the case for the mass parameters, which dimensionally tend to 'cancel' out in the coupling terms. For this reason changes in the mass parameters, as opposed to changes in length, have less of an effect on the overall coupling strength. This trend has been confirmed by numerical simulations.

Secondly, it is required in order to calculate the Lyapunov exponents accurately. The maximal Lyapunov exponent provides a quantitative measure of a non-linear system's sensitivity to initial conditions. Although a variety of methods have been developed for the accurate computation of Lyapunov exponents [12, 13], they invariably require analytical expressions for all the elements of the Jacobian matrix

$$J_{jk}(\mathbf{x}) = \frac{\partial f_j}{\partial x^k} \quad (j, k = 1, \dots, 6) \tag{3}$$

In dynamical systems for which the analytical expressions are not know, the Lyapunov exponents can be estimated by, for example, fitting the time series with an analytical function through least square minimisation [14]. Note that it is not sufficient to calculate the Jacobian matrix numerically, because the sensitivity to numerical errors in calculations of this nature is extreme. Therefore, in this work, equations (A.1) to (A.6) were used to obtain the required analytical expressions for the Jacobian matrix.

3. Computational aspects and visualisation

A visualisation of the pendulum was developed in the *Python* programming language [11], using the *Visual* module. In order to improve the efficiency of the numerical calculations, which involve solving the system (2) in real time, the numerically intensive parts of the calculation were first coded as two separate Fortran 90 subroutines. The first subroutine was used to calculate the Lyapunov exponents according to the method of Chen *et al.* [13], and the second to integrate the system of equations by calling the ISML subroutine *dverk.f90*. Note that the first subroutine makes calls to the second in order to integrate the linearized system of $n(n+1)$ equations ($n = 6$) and returns the Lyapunov exponents in base e, as is the modern convention. A shared library of the two main subroutines was created by using *f2py* [15]. *Scipy.optimize* was imported to perform downhill simplex optimisation via the function *fmin* [16].

4. Results and discussion

In this section two examples of the optimisation technique are provided. In both examples the starting parameter values and initial conditions were arbitrarily chosen and are the same for both examples.

In the first, a periodic mode of the pendulum was calculated, with the result shown in figure 2. This mode was obtained by optimising the initial conditions, with the starting parameters fixed. After optimisation all the Lyapunov exponents were equal to zero, within the set numerical tolerance of $\lambda_{max} \leq 10^{-3}$.
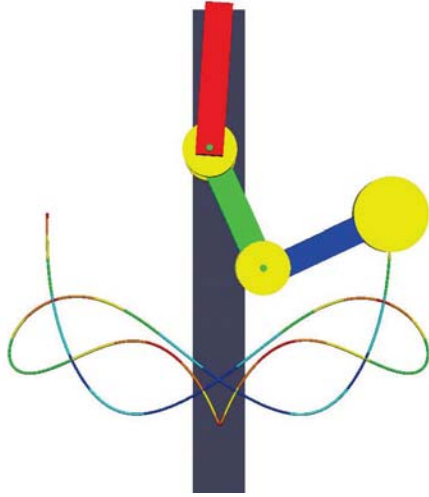
Figure 2. A periodic mode of the un-damped pendulum obtained through optimisation of the initial condition. In this figure the parameter values are $\ell_1 = \ell_2 = \ell_3 = 0.1\,\mathrm{m}$ and $m_1 = m_2 = m_3 = 0.1\,\mathrm{kg}$. The starting initial condition was arbitrarily chosen as $x_1 = x_2 = x_3 = 1.5$, with all the initial velocities constrained to zero. The optimised initial condition, which produces the periodic motion shown, was obtained by demanding $\lambda_{\mathrm{max}} \leq 0.001$. The optimised initial condition was found to be $x_1 = -0.06113$, $x_2 = 0.42713$ and $x_3 = 2.01926$.

In the second example a an extreme hyperchaotic mode was calculated, with the result shown in figure 3. This mode was obtained by fixing the initial condition and optimising only the lengths
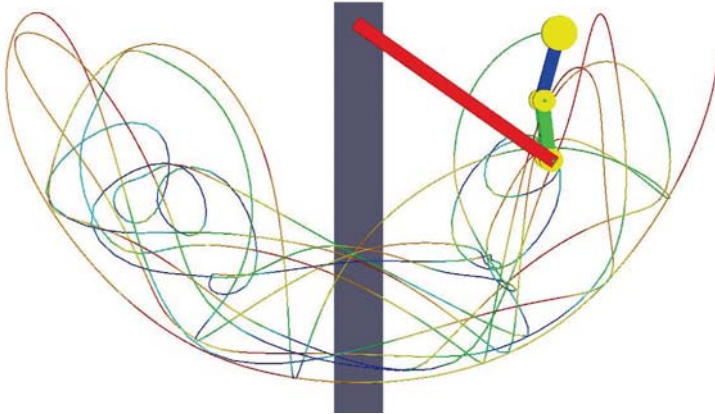
Figure 3. A hyperchaotic mode of the un-damped pendulum obtained through optimisation of the parameters. The initial condition and starting parameter values were the same as in figure 1. Note that, in both figures, one of the two pedestals (shown in gray) has been removed in order to display the trajectory followed by the centre of m_3 more clearly.

and masses. In view of the analysis given just after equation (2), high values of the Lyapunov exponents were expected for very small lengths. Indeed, in searching for optimised parameter sets for the hyperchoatic modes of the pendulum, it was found that the lengths had to be constrained to remain greater than zero. In this example the lengths were thus arbitrarily constrained to be greater than $0.050\,\mathrm{m}$ in order to ensure that the optimised system is physically realisable. Optimisation of all six parameters could then be used to change the Lyapunov exponents from their initial values of $\lambda_1 = 4.58$ and $\lambda_2 = 1.81$ (already hyperchaotic) to a predefined much higher value of (in this example) $\lambda_1 > 10.0 \pm 0.1$. The optimised parameters were found to be $m_1 = 0.106\,\mathrm{kg}$, $m_2 = 0.098\,\mathrm{kg}$, $m_3 = 0.123\,\mathrm{kg}$, $\ell_1 = 0.187\,\mathrm{m}$, $\ell_2 = 0.050\,\mathrm{m}$ and $\ell_3 = 0.051\,\mathrm{m}$. The corresponding Lyapunov exponents were $\lambda_1' = 10.06$, $\lambda_2' = 1.85$ and $\lambda_3' = 0.00$. In other calculations, which are not reported here, it was possible to optimise the parameters and initial conditions simultaneously.

The above results are significant because there are relatively few real physical systems that can be classified as hyperchaotic, with Lyapunov exponents in the range 2-3 or above.

5. Conclusion

The preliminary results reported in the present work show that the triple pendulum system is hyperchaotic, and that its degree of chaos can be controlled through optimisation.

Although the method is based on the result of memory intensive algebraic simplifications of the governing equations, it has the advantage of providing control over the Lyapunov exponents. As examples of its use, the initial conditions for periodic motion (usually obtained via the less efficient shooting method) were obtained and the maximal Lyapunov exponent of the same system was enhanced by more than a factor of 2 by optimisation of the parameters alone.

The present article lays the theoretical and numerical foundation for a future in-depth analysis of the hyperchaotic triple pendulum system. It provides an optimisation method that offers precise control over the Lyapunov exponents. Such control may also be useful in a wide variety of other non-linear applications, such as those occuring in biophysics and electrical engineering (encryption).

Appendix A. Equations of motion

$$\dot{x}_1 = x_4 \tag{A.1}$$

$$\dot{x}_2 = x_5 \tag{A.2}$$

$$\dot{x}_3 = x_6 \tag{A.3}$$

$$
\begin{aligned}
\dot{x}_4 = {} & \frac{\ell_2 \ell_3 g}{4D} \Big[m_1 m_3^2 \left(\sin\left(x_1 - 2x_2 + 2x_3 \right) + \sin\left(x_1 + 2x_2 - 2x_3 \right) \right) \\
& -2 \left(m_2^2 m_3 + m_2 m_3^2 \right) \sin\left(x_1 - 2x_2 \right) \Big] \\
& - \frac{\ell_2 \ell_3 g}{2D} m_3 \left(2m_1 m_2 + m_1 m_3 + m_2 m_3 + m_2^2 \right) \sin x_1 \\
& - \frac{\ell_1 \ell_2 \ell_3}{2D} \left(m_2 m_3^2 + m_2^2 m_3 \right) x_4^2 \sin\left(2x_1 - 2x_2 \right) \\
& - \frac{\ell_2^2 \ell_3}{D} \left(m_2 m_3^2 + m_2^2 m_3 \right) x_5^2 \sin\left(x_1 - x_2 \right) \\
& - \frac{\ell_2 \ell_3^2}{2D} m_2 m_3^2 x_6^2 \left(\sin\left(x_1 - x_3 \right) + \sin\left(x_1 - 2x_2 + x_3 \right) \right) + \chi_1
\end{aligned}
\tag{A.4}
$$

$$
\begin{aligned}
\dot{x}_5 = {} & \frac{\ell_1 \ell_3 g}{4D} \left(2m_1 m_2 m_3 + m_1 m_3^2 + 2m_2 m_3^2 + 2m_2^2 m_3 \right) \left(\sin\left(2x_1 - x_2 \right) - \sin x_2 \right) \\
& - \frac{\ell_1 \ell_3 g}{4D} m_1 m_3^2 \left(\sin\left(x_2 - 2x_3 \right) + \sin\left(2x_1 + x_2 - 2x_3 \right) \right) \\
& + \frac{\ell_1^2 \ell_3 m_3}{2D} \Big[\left(2m_1 m_2 + m_1 m_3 + 2m_2 m_3 + 2m_2^2 \right) x_4^2 \sin\left(x_1 - x_2 \right) \\
& - m_1 m_3 x_4^2 \sin\left(x_1 + x_2 - 2x_3 \right) \Big] \\
& + \frac{\ell_1 \ell_2 \ell_3}{2D} \left(\left(m_2 m_3^2 + m_2^2 m_3 \right) x_5^2 \sin\left(2x_1 - 2x_2 \right) - m_1 m_3^2 x_5^2 \sin\left(2x_2 - 2x_3 \right) \right)
\end{aligned}
\tag{A.5}
$$

$$-\frac{\ell_1\ell_3^2}{2D}\left(\left(2m_1m_3^2+m_2m_3^2\right)x_6^2\sin\left(x_2-x_3\right)-m_2m_3^2x_6^2\sin\left(2x_1-x_2-x_3\right)\right)+\chi_2$$

$$
\begin{aligned}
\dot{x}_6 &= \frac{\ell_1\ell_2 g}{4D}\left(m_1m_2m_3+m_1m_3^2\right)\left(\sin\left(2x_1-x_3\right)+\sin\left(2x_2-x_3\right)\right) \qquad\text{(A.6)}\\
&\quad -\frac{\ell_1\ell_2 g}{4D}\left(m_1m_2m_3+m_1m_3^2\right)\left(\sin\left(2x_1-2x_2+x_3\right)+\sin x_3\right)\\
&\quad +\frac{\ell_1^2\ell_2}{2D}\left(m_1m_2m_3+m_1m_3^2\right)x_4^2\left(\sin\left(x_1-x_3\right)-\sin\left(x_1-2x_2+x_3\right)\right)\\
&\quad +\frac{\ell_1\ell_2^2}{D}\left(m_1m_2m_3+m_1m_3^2\right)x_5^2\sin\left(x_2-x_3\right)\\
&\quad +\frac{\ell_1\ell_2\ell_3}{2D}m_1m_3^2x_6^2\sin\left(2x_2-2x_3\right)+\chi_3
\end{aligned}
$$

where $g = 9.81\,\mathrm{ms}^{-2}$ is the gravitational acceleration and

$$
\begin{aligned}
D &= \frac{\ell_1\ell_2\ell_3}{2}m_3\left[\ 2m_1m_2+m_1m_3+m_2m_3+m_2^2-m_2\left(m_2+m_3\right)\cos\left(2x_1-2x_2\right)\right.\\
&\quad \left.-m_1m_3\cos\left(2x_2-2x_3\right)\ \right]
\end{aligned}
$$

In equations (A.4) to (A.6), χ_1, χ_2 and χ_3 represent additional terms; such as, those proportional to the damping coefficients c_1, c_2 and c_3, or in the case of a physical pendulum, the additional terms involving moments of inertia. When the upper link of the pendulum is driven by a harmonic force the six equations have to be supplemented by a seventh, namely $\dot{x}_7 = \omega$, where ω is the angular frequency of the driving force [9]. The driving force also introduces additional terms which are not included here in order to reduce the length of the printed expressions.

References

[1] Awrejcewicz J and Lamarque C H 2003 *World Scientific Series on Nonlinear Science (Series A* vol 45) ed Chua L O (Singapore: World Scientific)

[2] Eltohamy K G and Kuo C 1999 *International Journal of Systems Science* **30** 505

[3] Furata T, Tawara T, Okumura Y, Shimizu M and Tomiyama K 2001 *Robotics Autonomous Systems* **37** 81

[4] de Paula A S, Savi M A, and Pereira-Pinto F H I 2006 *Journal of Sound and Vibration* **294** 585

[5] Gitterman M 2010 *The Chaotic Pendulum* (Singapore: World Scientific)

[6] Plissi M V, Torrie C I, Husman M E, Robertson N A, Strain K A, Ward H, Lück H and Hough J 2000 *Review of Scientific Instruments* **71** 2539

[7] Awrejcewicz J and Kudra G 2005 *Nonlinear Analysis* **63** 909

[8] Awrejcewicz J, Supel B, Lamarque C H, Kudra G, Wasilewski G and Olejnik P 2008 *International Journal of Bifurcation and Chaos* **18** 2883

[9] Awrejcewicz J, Kudra G and Lamarque C H 2004 *International Journal of Bifurcation and Chaos* **14** 4191

[10] Kudra G 2002 *Analysis of Bifurcation and Chaos in Triple Physical Pendulum with Impacts* Ph.D. thesis Technical University of Lódź

[11] Chun W J 2007 *Core Python Programming* 2nd ed (New Jersey: Prentice Hall)

[12] Wolf A, Swift J B, Swinney H L and Vastano J A 1985 *Physica D* **16** 285

[13] Chen Z M, Djidjeli K and Price W G 2006 *Applied Mathematics and Computation* **174** 982

[14] Sattin F 1997 *Computer Physics Communications* **107** 253

[15] Langtangen H P 2004 *Python Scripting for Computational Science* (Berlin: Springer Verlag)

[16] Nelder J A and Mead R 1965 *Computer Journal* **7** 308 Also see *www.scipy.org*